Stationary Waves of the Ice Age Climate

KERRY H. COOK AND ISAAC M. HELD

Geophysical Fluid Dynamics Laboratory/NOAA, Princeton University, Princeton, New Jersey

(Manuscript received 28 December 1987, in final form 25 April 1988)

ABSTRACT

A linearized, steady state, primitive equation model is used to simulate the climatological zonal asymmetries (stationary eddies) in the wind and temperature fields of the 18 000 YBP climate during winter. We compare these results with the eddies simulated in the ice age experiments of Broccoli and Manabe, who used CLIMAP boundary conditions and reduced atmospheric CO_2 in an atmospheric general circulation model (GCM) coupled with a static mixed layer ocean model. The agreement between the models is good, indicating that the linear model can be used to evaluate the relative influences of orography, diabatic heating, and transient eddy heat and momentum transports in generating stationary waves. We find that orographic forcing dominates in the ice age climate. The mechanical influence of the continental ice sheets on the atmosphere is responsible for most of the changes between the present day and ice age stationary eddies. This concept of the ice age climate is complicated by the sensitivity of the stationary eddies to the large increase in the magnitude of the zonal mean meridional temperature gradient simulated in the ice age GCM.

1. Introduction

Large orographic features, such as the Tibetan Plateau, the Rocky Mountains and, presumably, the continental ice sheets of the ice age climate, generate zonal asymmetries in the atmospheric circulation. These planetary-scale features of the climate, which are often referred to as stationary eddies or stationary waves, are also generated by zonal asymmetries in the transient eddy transports of heat and momentum and by asymmetries in diabatic heating. One of the major challenges of dynamic meteorology is to relate the observed stationary waves to these forcing functions and, ultimately, to the surface boundary conditions. An understanding of stationary waves is central to studies of regional climates and their responses to changes in boundary conditions. In this study we test linear theory by comparing the generation of stationary waves by a linear model with results from a general circulation model (GCM) of the Northern Hemisphere winter during the Last Glacial Maximum 18 000 years ago. We then use the linear model as a diagnostic tool to explore the relationship between the simulated stationary waves and the forcing functions in the GCM's ice age climate.

The steady response to a given zonally asymmetric forcing is computed by a linear model using dynamical and thermodynamical equations linearized about a given zonally symmetric climate. Multilevel linear models based on the primitive equations have evolved from the barotropic and quasi-geostrophic models of Charney and Eliassen (1949) and Smagorinsky (1953). An important step in the recent development of this subject is the recognition of the crucial importance of spherical geometry and the meridional propagation of Rossby waves in addition to zonal and vertical propagation. For a discussion of the relevant theory, refer to the seminal paper by Hoskins and Karoly (1981) and the review by Held (1983). Jacqmin and Lindzen (1985) and Chen and Trenberth (1987) have made encouraging attempts to simulate the stationary wave patterns observed during the present day Northern Hemisphere winter using observations to define the basic zonally symmetric climate state and the forcing functions. One limitation of these studies is that the distributions of diabatic heating and transient eddy fluxes in the atmosphere are not known with any precision. This hampers linear model studies because it can be unclear whether discrepancies between the modeled and observed stationary waves are caused by nonlinear interactions or simply by errors in the forcing fields.

To avoid this problem, Nigam et al. (1986, 1988) use a general circulation model (GCM) as a surrogate atmosphere and a linear model designed to be compatible with the GCM. Forcing and zonal mean fields can be specified exactly from any GCM climatology. A result from Nigam et al. (1988) illustrates the potential of linear stationary wave theory. The linear model result for the wintertime, orographically forced, stationary eddy geopotential at 300 mb is on the left in Fig. 1. (According to this model, orographical forcing is responsible for about two-thirds of the geopotential

Corresponding author address: Dr. Kerry H. Cook, NOAA/GFDL, Princeton University, P.O. Box 308, Princeton, NJ 08542.

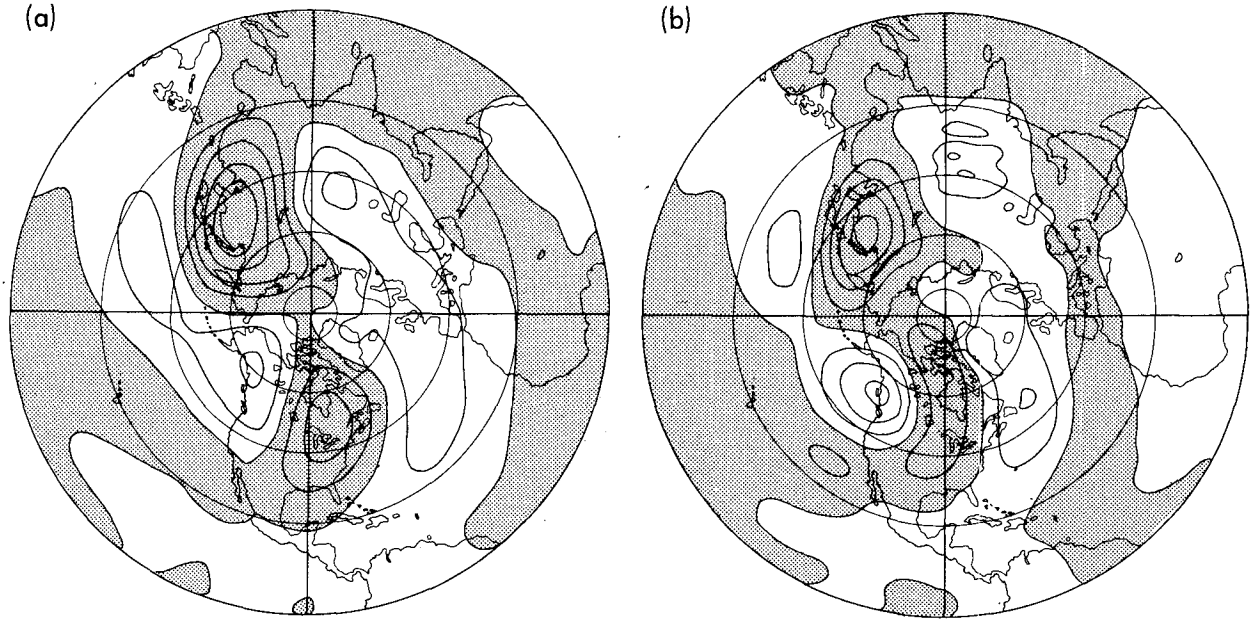

FIG. 1. (a) Wintertime stationary eddy geopotential at 300 mb predicted by the linear model forced by orography and linearized about the zonal mean fields in a GCM with prescribed ocean temperature. (b) The difference in the stationary eddy 300 mb geopotential between two GCM's with fixed ocean temperatures, one with and one without mountains. Contour interval is 40 gpm and negative values are shaded.

signal at this level.) The right half of Fig. 1 shows the difference between the stationary wave patterns from two GCM integrations—one with realistic orography and one with a flat surface. The good agreement suggests that the linear model can provide useful approximations to the orographic component of a GCM's stationary wave field.

The linearity of the response to diabatic heating and transient eddies is less clear. Nigam et al. (1986) consider a GCM with a flat lower boundary and find that diabatic heating and transient eddies force a stationary wave pattern in the linear model in good agreement with the GCM. There is, however, considerable compensation between the responses to low-level transients and extratropical heating, suggesting that these forcing functions are not independent and that the linear decomposition of the flow into separate parts forced by heating and transients may not be robust. In experiments with realistic orography (Nigam et al. 1988), the response is less satisfactory, especially at low levels. This may be due to nonlinear interactions between the thermally and orographically induced waves. One form of this type of interaction has been recently analyzed by Chen and Trenberth (1987). Of course, the formidable problem of relating the diabatic heating and transient eddy forcing functions to the boundary conditions remains.

Although there are many unknowns concerning the limitations of linear stationary wave theory, results as in Fig. 1 encourage us to analyze the climate of the Last Glacial Maximum (18 000 years before present) in a similar way. The Laurentide ice sheet covered much of North America during this period. It must have been responsible for a stationary wave pattern that was an important, if not dominant, feature of the ice age atmosphere. In this paper we investigate how these waves are forced by a prescribed ice age topography and what their structure implies about the ice age climate. We do not address the influence of the stationary waves on the maintenance of the ice sheets. (See, however, Lindeman and Oerlemans 1987.)

Modeling the ice age atmosphere is possible because the CLIMAP Project (1976, 1981) reconstructed features of the ice age climate that are used as boundary conditions in GCMs. As a result, a number of models have been applied to this problem. Gates (1976), Kutzbach and Guetter (1986), and Rind (1987) conducted GCM experiments with the CLIMAP sea surface temperatures prescribed at the surface. Manabe and Broccoli (1985a,b) and Broccoli and Manabe (1987) used an atmospheric GCM coupled to a mixed layer ocean model in an ice age experiment, allowing them to simulate the ice age sea surface temperatures and isolate the influence of the ice sheets on the surface temperature as well as the flow fields.

We use Broccoli and Manabe's (1987) simulations of the ice age climate to define the basic zonal state and forcing functions for the linear model. The stationary eddies simulated by the GCM serve as a standard of comparison for the linear simulation. These GCM calculations indicate that the strong surface cooling over the North Atlantic that is the hallmark of the ice age climate is related to the presence of the Laurentide ice sheet. The ice sheet boundary conditions

result in several changes in the external forcing of the model climate, including the radiative, sensible, and latent heat fluxes at the surface. But the elevation of the land surface seems to be the most important, at least in winter. With the linear model we can study these forcings individually.

In section 2, the GCM experiments and the linear model are described briefly. The ability of the linear model to simulate the differences in the stationary waves between the ice age and present day climates is examined in section 3. In section 4 we explore how the ice age stationary wave amplitudes depend on changes in the zonal-mean climate, and in section 5 we address the implications of these results for our understanding of the ice age climate.

2. Models and experiments

The GCM data for the zonal mean and forcing fields are taken from a series of four integrations described by Broccoli and Manabe (1987). The lower boundary conditions include realistic continents and orography, with the oceans represented by a fixed depth (50 m) static mixed layer. The GCM is a low-resolution spectral model, with rhomboidal-15 truncation that is equivalent to a transform-grid resolution of about 4.5° lat and 7.5° long. Insolation varies seasonally, but not diurnally. Sea ice extent is calculated as a result of the surface heat balance over the oceans and clouds are fixed at their observed seasonal and zonal-mean values at each latitude and height. The effects of fixing the cloud distribution for the ice age application are discussed in Manabe and Broccoli (1985b).

Broccoli and Manabe (1987) describe four GCM integrations: 1) present day; 2) ice sheet only; 3) ice sheet plus land albedo; and 4) full ice age. The present day and full ice age simulations have four differences in boundary conditions: the distribution of continental ice; atmospheric CO_2 concentration; the continental outlines, which are modified due to the change in sea level; and snow-free land albedos, which reflect differences in vegetation types and ranges. The continental ice distribution, snow-free land albedos, and sea level are based on the CLIMAP reconstruction, while the CO_2 concentration is reduced from 300 to 200 ppmv for the ice age simulation according to the measurements of Neftel et al. (1982) and Shackleton et al. (1983). The changes in orography due to the presence of huge ice sheets in North America and Scandinavia are especially relevant for this study. Figure 2 shows the ice age orography in the Northern Hemisphere. More detail about the ice age boundary conditions and their effects on the GCM's climate, especially near the surface, is included in Broccoli and Manabe (1987).

Despite the fact that changes in the surface albedo due to the presence of the ice sheets are larger during the summer in the Northern Hemisphere, the ice sheets exert their most significant influence on the stationary waves during Northern Hemisphere winter when strong zonal winds pass over the Laurentide ice sheet. For this reason we consider Northern Hemisphere winter only, and use GCM data averaged over the 15 winter months (DJF) from the last 5 yr of each integration.

Large changes in the GCM's stationary waves occur when the ice age boundary conditions are introduced. Figure 3a shows the Northern Hemisphere wintertime eddy geopotential, i.e., the geopotential with the zonal mean removed, at 300 mb for the present day model climate. The full ice age case, with CLIMAP boundary conditions and reduced atmospheric CO_2, is in Fig. 3b. There is a planetary-scale stationary wave associated with the Tibetan Plateau in both cases, and a second wave train in the ice age case that is associated with the Laurentide ice sheet. When this stationary wave pattern is added to the zonally averaged flow, the result is the split jet stream over North America described by Manabe and Broccoli (1985). The amplitude of the dominant low in the Tibetan wave train is about 240 gpm in the present day simulation, and 160 gpm in the ice age simulation. The ice age stationary wave in the western hemisphere is the largest perturbation, reaching 280 gpm in the high over western Canada. These are the features of the GCM's climate that we wish to simulate and study with the linear model.

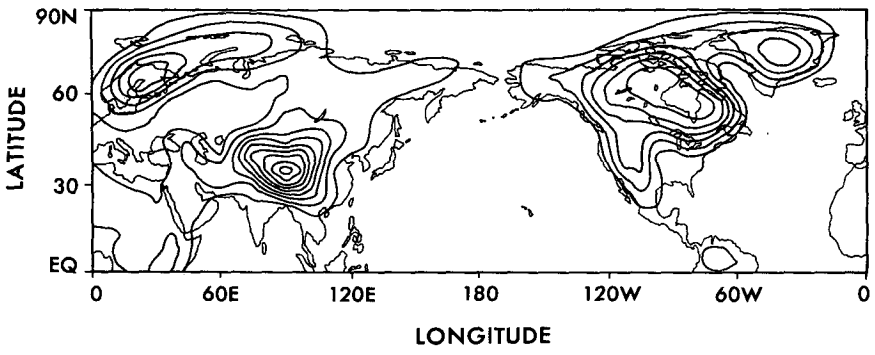

FIG. 2. Northern Hemisphere topography from CLIMAP. Contours are 500 m, and the land/sea distribution drawn is for the present day.

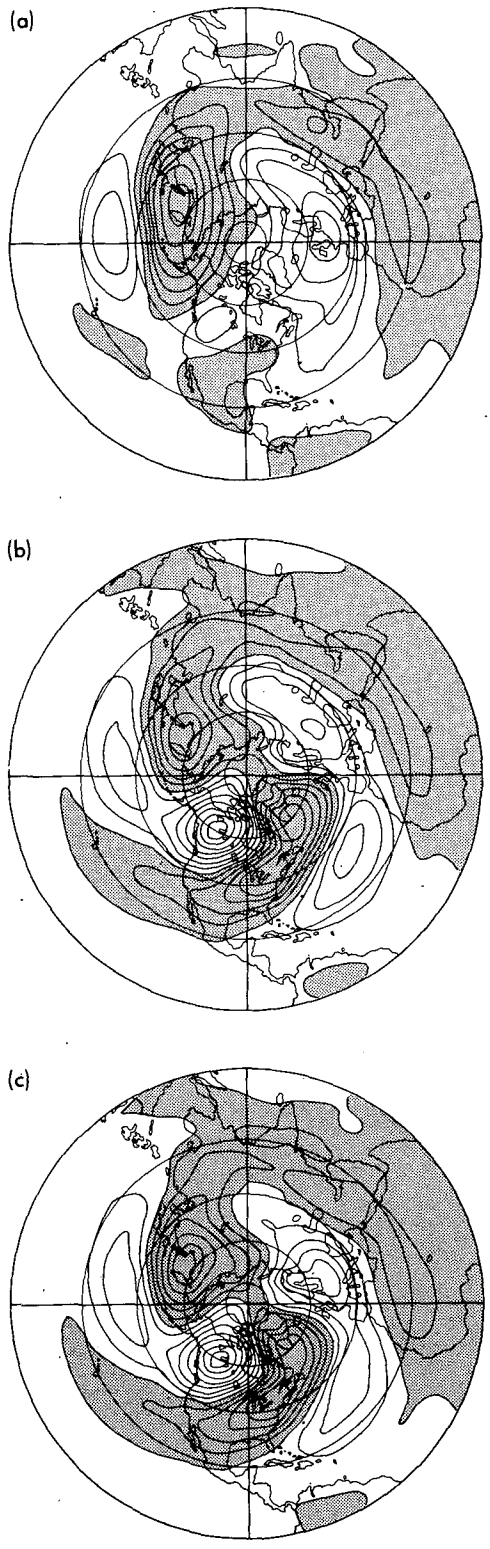

FIG. 3. Northern Hemisphere wintertime eddy geopotential at 300 mb from the GCM experiments of Broccoli and Manabe (1987) for the (a) present day, (b) full ice age and (c) ice sheet only climatologies. Contour interval is 40 gpm and negative values are shaded.

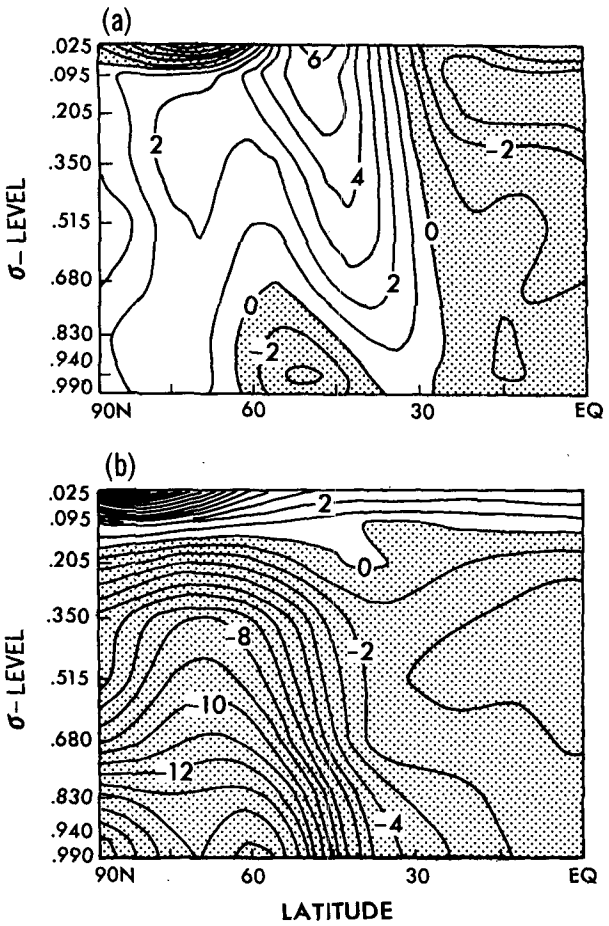

FIG. 4. Differences in the Northern Hemisphere (a) zonal mean zonal wind (1 m s^{-1} contours) and (b) temperature (1 K contours) in the GCM as a function of latitude and σ-level. Values are for "ice age" minus "present day."

Figure 3c shows the 300 mb eddy geopotential for the GCM experiment with ice sheets, but without reduced CO_2 and CLIMAP land albedos. The results are similar to the full ice age case of Fig. 3b, especially in the western hemisphere. The differences between Figs. 3b and 3c are largely due to the CO_2 decrease which seems to amplify the effect of the ice sheets on the eddies, but not change their structure significantly. Changes in bare land albedos play a minor role in establishing this pattern.

The zonal mean zonal winds and temperatures on σ-surfaces are required as inputs for the linear model. Differences in these fields between the GCM equilibria—"ice age" minus "present day"—are shown in Fig. 4. The zonal wind is smaller at all altitudes in the tropical troposphere in the ice age climate, and generally larger in midlatitudes (Fig. 4a). The slower winds below $\sigma = 0.680$ near 50°N latitude are probably related to the presence of the Laurentide ice sheet. Away from the ice sheets, in the tropics and subtropics, the zonal

wind changes are similar in both hemispheres. One obtains similar results if one computes zonal averages along pressure surfaces, taking care at low levels to average only over those regions where a given pressure surface exists. The response of the linear model is not changed significantly if one linearizes about a basic state obtained by averaging along pressure rather than σ-surfaces.

General tropospheric cooling is evident in the zonal mean temperature change (Fig. 4b), with maxima at high latitudes near the surface. At the latitude of the Laurentide ice sheet, the zonal mean temperature near the surface is 15 K cooler in the ice age case. The temperature difference directly south of the ice sheet turns out to be particularly important for studying changes in stationary waves in response to ice age boundary conditions. Between 45° and 60°N, the magnitude of the zonal mean meridional temperature gradient near the surface doubles in the Northern Hemisphere.

Three types of forcing can be used to induce zonal asymmetries in the linear model—orographic forcing, thermal forcing, and transient eddy forcing. They can be included individually or in any combination. Orographic forcing can be thought of as the imposition of a vertical velocity at the lower boundary given by the product of the zonal mean zonal wind and the longitudinal derivative of the surface height. A mountain should be thought of as infinitesimal in the linear model in that it does not represent a physical barrier to the flow as in the GCM. The three-dimensional thermal and transient eddy forcing fields include latent, sensible and radiative heating, and horizontal momentum and heat transport by transient eddies at each of the nine σ-levels. Experiments with the linear model suggest that momentum fluxes play a minor role in the differences between ice age and present day stationary waves, and we do not discuss them further. Diabatic heating and heat transport by transient eddies play a more significant role, especially near the surface. Figure 5a shows the difference between the ice age and present day dia-

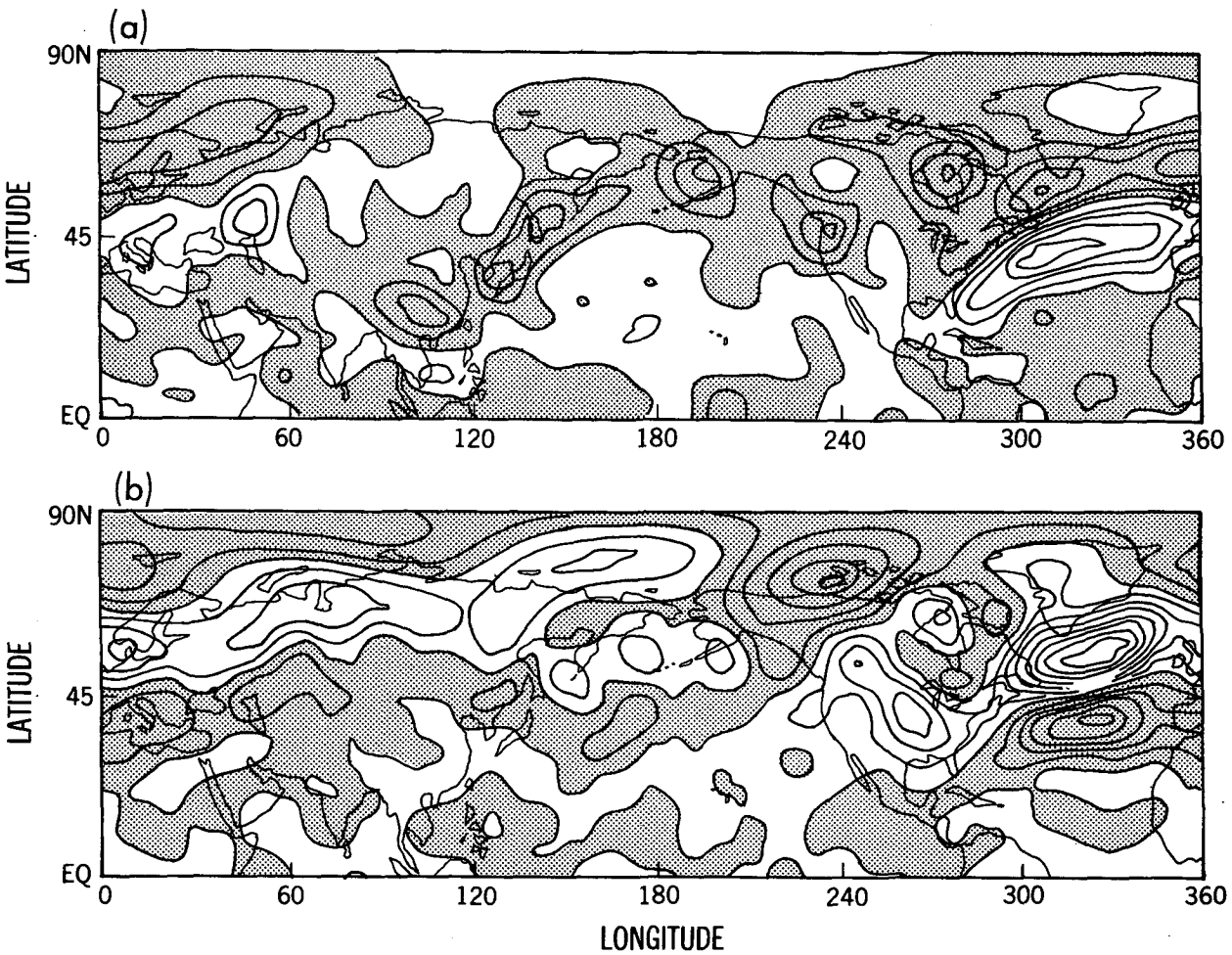

FIG. 5. Differences ("ice age" minus "present day") in the GCM's (a) diabatic heating and (b) transient eddy heat flux convergence averaged over the lower troposphere ($\sigma > 0.575$). Contours are 0.25 K day^{-1}. Shaded values are negative.

batic heating (latent plus sensible plus radiative heating) averaged over the lower troposphere, from the surface to 515 mb. The unshaded region over the Atlantic indicates an increase in the heating of the atmosphere by the ice age ocean due to the much colder air in this region. Increases in the sensible heat flux are largely responsible for the increased atmospheric heating in this region. The ice line moves south to about 55°N in the ice age case, cutting off direct sensible heat transfer over the northern North Atlantic. The low-albedo ocean surface is replaced with high-albedo ice that insulates the atmosphere from the warm ocean, causing cooling over the Atlantic at high latitudes.

Figure 5b shows changes in the heat flux convergence by transient eddies vertically averaged over the lower troposphere. These forcing functions are calculated as a residual from the GCM's time-averaged thermodynamic equation. Not surprisingly, the largest changes in the temperature tendency due to transients occur in the lower troposphere over North America and the North Atlantic. These changes are due to the larger heat flux by transient eddies in the enhanced Atlantic storm track. The tendency is out of phase with, and larger than, the diabatic heating changes in this region. Since these tendencies are apparently correlated in some regions, it makes little sense to use a linear model to simulate the effects of the heating modification on the circulation pattern without simultaneously considering the modified transient fluxes.

The linear model solves, by matrix inversion, for the deviations from the given zonal means of the surface pressure, and of winds and temperature at each of nine vertical levels that match those of the GCM. Longitudinal derivatives are treated spectrally as in the GCM, with 15 waves retained. For computer efficiency in the matrix inversion, the linear model is not fully spectral. Finite differencing on a staggered grid with a resolution of 1.8° is used to model meridional dependence. A detailed description can be found in Nigam (1983). We set the zonal mean meridional wind to zero in the linear model. This does not have a major effect on the eddy pattern in midlatitudes, and it does not change our conclusions.

3. Results

a. Comparison of modeled stationary eddies

We first investigate the ability of the linear model to replicate the GCM's stationary wave patterns for the present day and ice age cases. In the figures, eddies are defined as deviations from the zonal mean, with negative values shaded. Data from the models are converted from σ- to p-surfaces before eddy fields are calculated.

Figure 6 shows the Northern Hemisphere linear model eddy geopotential fields at 300 mb for comparison with the GCM eddies of Fig. 3, with present day cases on the left and ice age cases on the right. The top figures (Figs. 6a and 6b) are the present day and ice age simulations with full forcing (orography, diabatic heating, and transient eddy transports of heat and momentum). The eddies in the figures on the bottom (Figs. 6c and 6d) are the linear responses to orography alone.

Comparing the present day linear simulation with full forcing (Fig. 6a) with the present day GCM simulation (Fig. 3a), we note a serious discrepancy in the western hemisphere. The linear simulation has a strong low centered over northern Canada and Greenland, but in the GCM there is little or no stationary wave in this region. This situation is especially curious because observations show a wintertime low centered over the Hudson Bay, with the 300 mb geopotential about 160 gpm less than the zonal mean. Since the linear model forced by fields from the GCM actually simulates a wave in this region, some nonlinear process in the GCM must be damping the signal.

The situation is much improved for the present day simulation in the eastern hemisphere. The eddies generated over the Tibetan Plateau in the two models are similar, with the maximum perturbation in the GCM eddy geopotential slightly larger than in the linear model at this particular level. The stationary wave generated over Tibet in the ice age case is slightly stronger in the linear model than in the GCM (compare Fig. 6b with Fig. 3b).

Agreement between the two models is also good in the ice age western hemisphere. The locations of the high and low over the continent are very similar. Downstream of the Laurentide ice sheet, the errors in the linear model (Fig. 6b) grow due to differences in the path of the dominant wave train, which does not curve equatorward as strongly as in the GCM simulation (Fig. 3b). The subtropical Atlantic high generated by the GCM is displaced by the linear model to Western Europe and North Africa as a result.

The linear model was run repeatedly with each of the three types of forcing—orography, diabatic heating, and transient heat and momentum transports—included separately to determine which were the most important. (In the linear model, of course, the eddy patterns caused by each forcing must sum to the pattern with all forcings included.) At this level in the atmosphere, orographic forcing dominates in both the present day and ice age cases. The 300 mb stationary eddy geopotential patterns with orographic forcing alone in the linear model appear in Figs. 6c and 6d. The similarities to the corresponding full-forcing cases are striking, especially in the ice age simulation where including the effects of thermal forcing and transient eddies actually seems to degrade the simulation. The linear orography-only experiments even capture the weakening of the low over Tibet that occurs when ice age conditions are imposed in the GCM.

Despite the discrepancy in the present day simulations, a comparison between Figs. 6a and 6c, and Figs. 6b and 6d, reveals the dominance of orographic forcing.

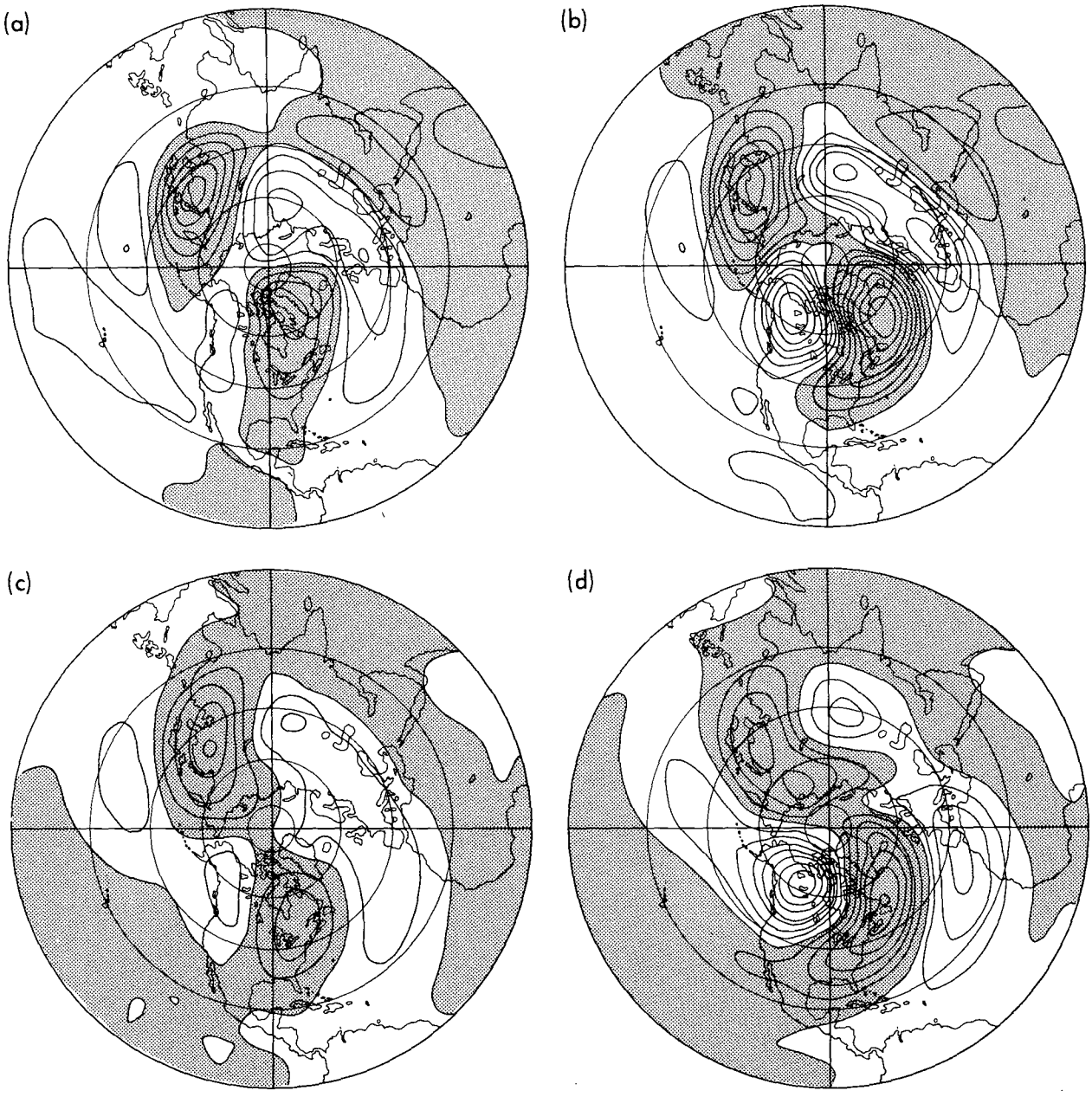

FIG. 6. Eddy geopotential at 300 mb from the linear model with (a) zonal mean fields and full forcing (see text) from the present day GCM, (b) zonal mean fields and full forcing from the ice age GCM, (c) present day GCM mean fields and orographic forcing alone, and (d) ice age GCM mean fields and orographic forcing alone.

In the western hemisphere during the ice age, the responses to thermal and transient eddy forcing tend to be out of phase, leaving the orographic response very similar to the full response. In the eastern hemisphere, including thermal and transient eddy forcing improves the agreement somewhat at high latitudes.

The linear model experiments confirm the conclusion from the GCM experiments that the continental ice is the dominant cause of the change in the stationary eddies in the ice age climate. In Broccoli and Manabe's "ice sheet only" experiment, the two distinct wave trains of the ice age atmosphere have nearly the same amplitude as in the full ice age experiment (see Figs. 3b and 3c). The linear model allows us to go a step further in the analysis of these waves and say that it is the direct mechanical effect of the ice sheet, as opposed to the changes in the heating field and transient eddies due to the presence of the ice sheet, that is largely responsible for the generation of these eddy patterns.

Figure 7 shows changes in the stationary eddy geo-

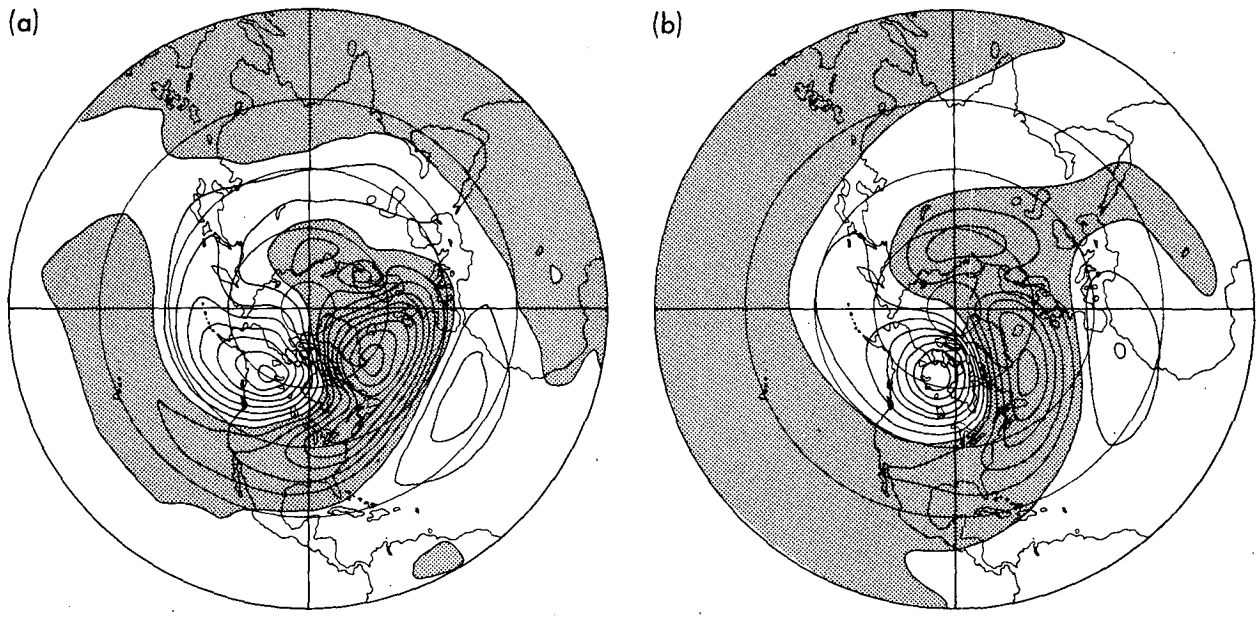

FIG. 7. Changes ("ice age" minus "present day") in the 300 mb eddy geopotential for the (a) GCM and (b) linear model with orographic forcing only. Contour interval is 40 gpm and negative values are shaded.

potential at 300 mb, "ice age" minus "present day," for the GCM full ice age experiment (Fig. 7a), and the linear model with orographic forcing alone (Fig. 7b). The differences in eddy amplitude over the North Atlantic (−320 gpm for the GCM vs −200 gpm for the linear model) are largely attributable to the distortion of the GCM's present day simulation. In the eastern hemisphere, the weakening of the Tibetan wave is evident in the GCM differences, where the positive region extends across the North Pacific and northern Asia. This weakening is less pronounced, but still present, in the linear model experiments.

In the standard GCM and linear model simulations positive eddy temperatures cover the North Atlantic below 500 mb. Near the surface, 4–6 K amplitudes in the subtropics increase to 8–10 K off the coast of Northern Europe. In the ice age simulations, the positive eddy temperatures of the northern North Atlantic are replaced by negative eddy temperatures. Figure 8 highlights the atmosphere at 940 mb over the North Atlantic, and shows eddy temperatures superimposed over the ice age continental outline as resolved by the GCM. Locations where the surface is above 940 mb in the GCM are blackened.

The GCM with full ice age boundary conditions is shown in Fig. 8a. The negative eddy temperatures approach their maximum values near the ice sheets. Comparing the full ice age and ice sheet only simulations indicates that the ice sheet accounts for about two-thirds of the amplitude of the eddies at this level, with the rest due to enhancement of the ice sheet effect by the reduced CO_2 concentration.

The linear response to ice age orography also results in a reversal of the sign of the eddy temperature at 940 mb in the North Atlantic (Fig. 8b). In this model, a single minimum of −10 K is centered over the ocean just south of Greenland. The positive eddy temperatures in the subtropical Atlantic are pushed farther south and east than in the GCM. The inclusion of diabatic heating and transient eddy forcing amplifies the perturbations, but also introduces significant "noise" at low levels. There is cancellation between the separate responses to heating and transient eddy fluxes in this region, so we do not believe their effect is as robust as the response to topography. A more complete model would include some theory for how the diabatic heating and transient eddy fluxes respond to the orographically forced eddy.

Figure 9 shows the "eddy winds" at 940 mb for the ice age North Atlantic in the GCM and the orographically forced linear model. The components of these vectors u' and v' are deviations from the zonal mean zonal wind and zonal mean meridional wind, respectively. In the GCM simulation (Fig. 9a) an anticyclone is generated over the subtropical Atlantic, with cyclonic motion over the North Atlantic south and east of the low in the eddy temperature. The flow of cold air from the north over the Laurentide and Greenland ice sheets' eastern slopes is evident in both the GCM and linear model (Fig. 9b) winds. A cyclone similar to the GCM's occurs in the linear simulation over the northern Atlantic. The anticyclone to the south is less well defined and displaced eastward with the positive eddy temperatures. This anticyclonic motion becomes better established higher in the linear model's troposphere. The difference in orientation of the linear model and GCM

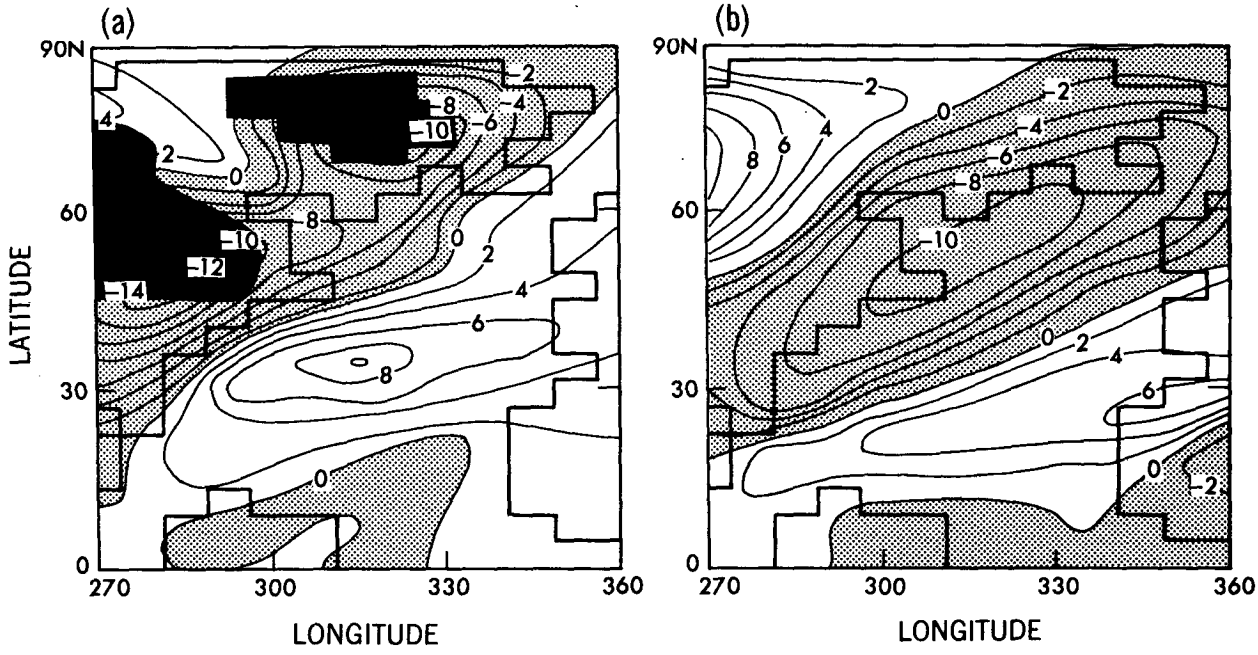

FIG. 8. Eddy temperatures at 940 mb for the (a) full ice age GCM, and (b) linear model with orographic forcing alone. Contour intervals are 2 K and negative values are shaded. Regions for which this pressure level does not exist in the GCM are blackened in panel (a). The continental outline is from CLIMAP as resolved by the GCM.

ray paths in the upper troposphere seen in Fig. 7 is reflected in this distortion of the low-level anticyclone in the linear model.

When forcing due to transient eddies and diabatic heating is added to the orographic forcing, the eddy winds are somewhat stronger in the lower troposphere. This does not improve or degrade the simulation of the ice age winds uniformly. The anticyclonic rotation over the subtropical Atlantic is not strengthened.

In general, the agreement between the wind simu-

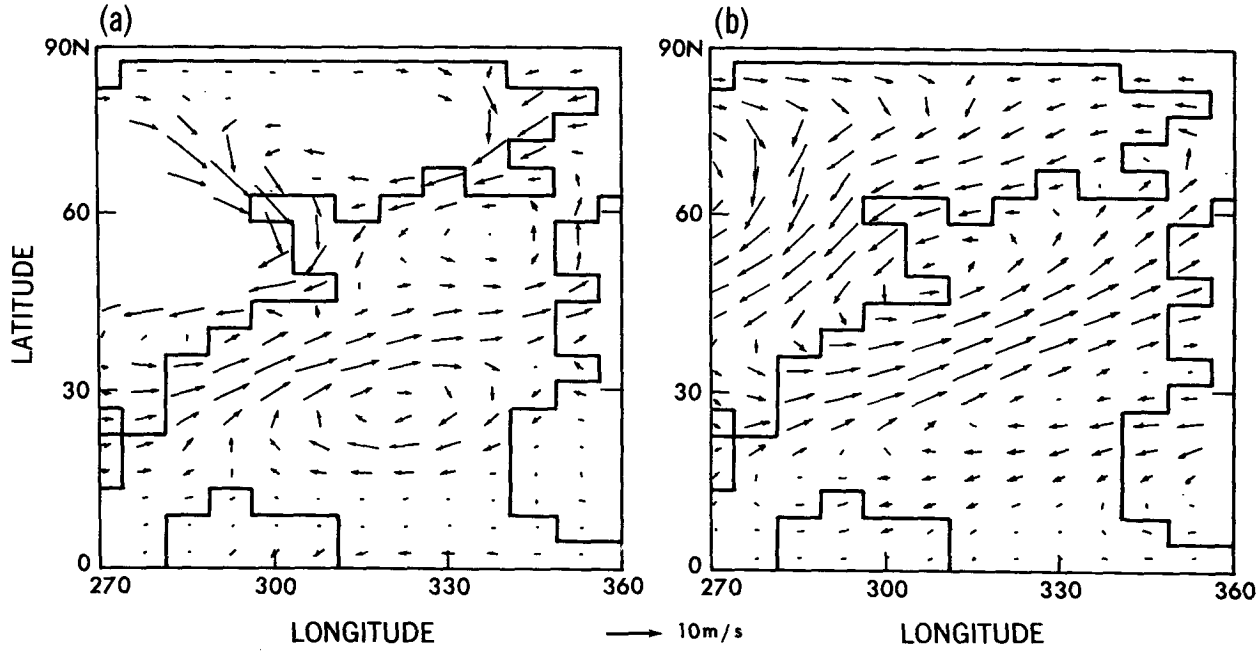

FIG. 9. Eddy winds at 940 mb for the (a) GCM with full forcing, and (b) linear model with orographical forcing alone. The scale is indicated by the arrow at the top of the figure.

lations degrades somewhat with proximity to the surface. One reason is that the GCM winds are interrupted by the physical presence of the orography. For example, the low level cold air advection over eastern Greenland is disrupted by the ice sheet in the GCM, but in the linear model the flow proceeds unchecked because the orography is effectively infinitesimal. Another reason is that in the vicinity of the low-level critical latitude near 30°N, where the zonal mean wind vanishes, the stationary linear solution becomes sensitive to the dissipation included in the model. It is not clear that the linear model's winds are sufficiently similar to the GCMs to justify using them to, say, estimate changes in the wind driven ocean circulation.

b. Importance of changes in the zonal mean flow

The linear model can be used to demonstrate that the changes in the basic zonal climate state shown in Fig. 4 are large enough to affect how the model atmosphere responds to orographic forcing. Figure 10a shows the linear response to ice age orography of the 300 mb eddy geopotential when the model is linearized about the zonally averaged basic state from the GCM's present day climatology. The stationary waves generated over the Laurentide ice sheet are much larger than when the GCM's ice age basic state is used (Fig. 6d), and much larger than in the ice age GCM (Fig. 3b). There is little change upstream so the amplification seems to occur on the downslope of the ice sheet. Similar, but less pronounced changes occur in the eastern hemisphere downstream of the Tibetan orography. The wave in Fig. 10a is so large that it could never be realized in the atmosphere or in a GCM; the wave would saturate by using up the existing mean gradients.

We can consider the change in the basic state flow as consisting of two parts: a change in the surface winds and a change in the vertical shear of the winds or, equivalently, in the horizontal temperature gradients. In Fig. 10b, the ice age zonal mean wind is restored in the lowest linear model layer ($\sigma = 0.99$), but the vertical shear of the wind and the temperature field are taken from the present day climate so that the thermal wind relation is not violated. The situation is not improved by this adjustment. The amplitude of the first low downstream of the major orographical features in both hemispheres is actually a bit larger than in the previous case (Fig. 10a). In Fig. 10c, the ice age temperature and vertical wind shear are used with the present day surface zonal wind. The results are very similar to the "correct" orographically forced waves of Fig. 6d. It appears that the changes in the zonal mean temperatures between the present day and ice age have the effect of damping the waves generated over the ice sheet.

To explore the influence of climatological changes in the zonal mean zonal winds and temperatures in more detail, consider the linearized, steady state thermodynamic equation. In the absence of diabatic heating and zonal mean vertical and meridional motion

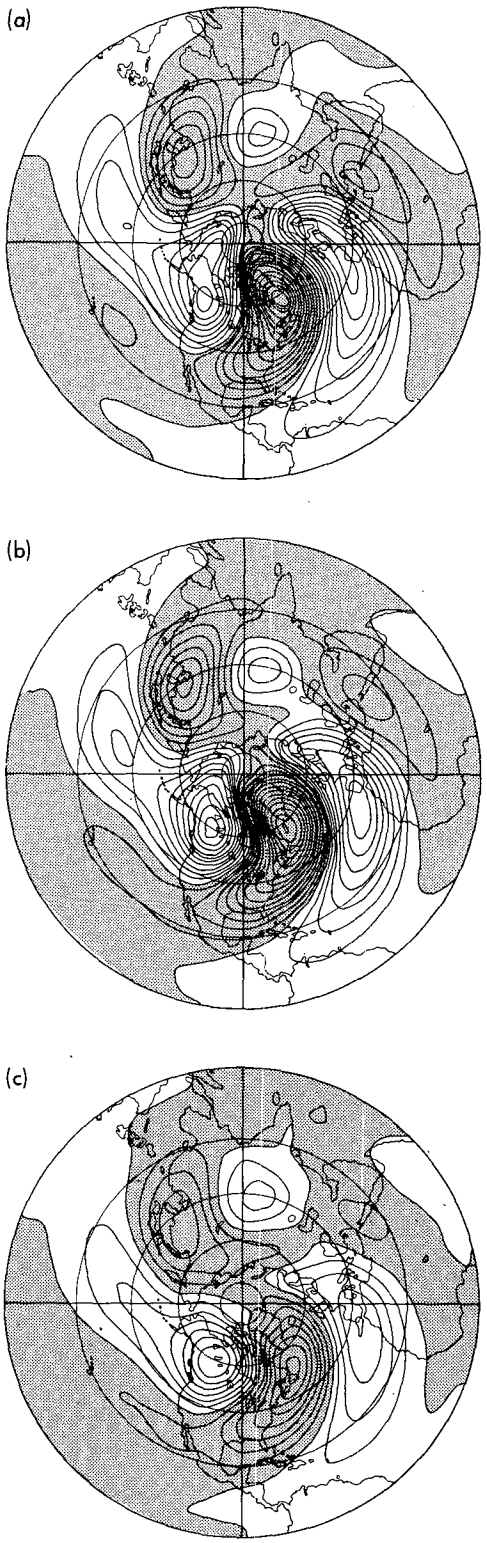

FIG. 10. Eddy geopotential at 300 mb for the linear model forced with ice age orography and linearized about (a) present day zonal mean fields, (b) present day temperature and ice age surface zonal wind, and (c) present day surface zonal wind and ice age temperatures (see text). Contour interval is 40 gpm.

$$\frac{\bar{u}}{a\cos\theta}\frac{\partial\Theta'}{\partial\lambda}+\frac{v'}{a}\frac{\partial\bar{\Theta}}{\partial\theta}=-w'\frac{\partial\bar{\Theta}}{\partial z}, \tag{1}$$

where Θ is potential temperature. (Overbars refer to the zonal mean and primes to deviations from zonal symmetry, i.e., $u=\bar{u}+u'$. Terms quadratic in the primed variables are neglected in the linearization.) At the surface,

$$w'=\mathbf{v}\cdot\nabla h\approx\frac{\bar{u}}{a\cos\theta}\frac{\partial h}{\partial\lambda} \tag{2}$$

where h is the deviation of the local height from the zonal mean. Then (1) becomes

$$\frac{\bar{u}}{a\cos\theta}\frac{\partial\Theta'}{\partial\lambda}+\frac{v'}{a}\frac{\partial\bar{\Theta}}{\partial\theta}=-\frac{\bar{u}}{a\cos\theta}\frac{\partial h}{\partial\lambda}\frac{\partial\bar{\Theta}}{\partial z}. \tag{3}$$

The roles of the zonal mean zonal wind, static stability, and zonal mean meridional temperature gradient are apparent in Eq. (3). If the first term dominates the left-hand side (LHS), then

$$\Theta'\approx -h(\partial\bar{\Theta}/\partial z). \tag{4}$$

Changes in the surface wind are irrelevant, and the increased stability of the ice age atmosphere is the only salient feature of the basic state modification. We expect the temperature perturbations to be in phase with the topography, with low temperature coincident with the top of the feature in a statically stable environment ($\partial\Theta/\partial z>0$). This balance predicts that an increase in the atmosphere's stability near the surface leads to an increase in the temperature perturbation. Since the ice age climate is more stable than the present day climate near the surface, this balance cannot explain why the ice age basic state reduces the amplitude of the stationary eddies.

If the second term on the left is important, then

$$v'\approx -\frac{\bar{u}}{\cos\theta}\frac{\partial h}{\partial\lambda}\frac{\partial\bar{\Theta}/\partial z}{\partial\bar{\Theta}/\partial\theta}=\frac{\bar{u}}{\cos\theta}\frac{\partial h}{\partial\lambda}\left(\frac{\partial z}{\partial\theta}\right)_{\Theta}^{-1} \tag{5}$$

where $(\partial z/\partial\theta)_\Theta$ is the slope of an isentropic surface. Changes in the zonal mean zonal wind and the isentropic slope at the surface effect the eddy meridional velocity perturbation, which will be in phase with the longitudinal gradient of the topography. Southward motion will occur on the lee side of an orographic feature given $\bar{u}>0$ and $\partial\Theta/\partial y<0$. Since our linear model results, in Fig. 10, clearly point to changes in the temperature field and not the surface wind as being of greatest importance, we must conclude that it is the increased meridional temperature gradient ($\partial\Theta/\partial\theta$) that causes the reduction in stationary wave amplitude.

For a direct investigation of the balance indicated in Eq. (3), the two terms on the LHS are drawn on pressure surfaces in Fig. 11 using the orographically

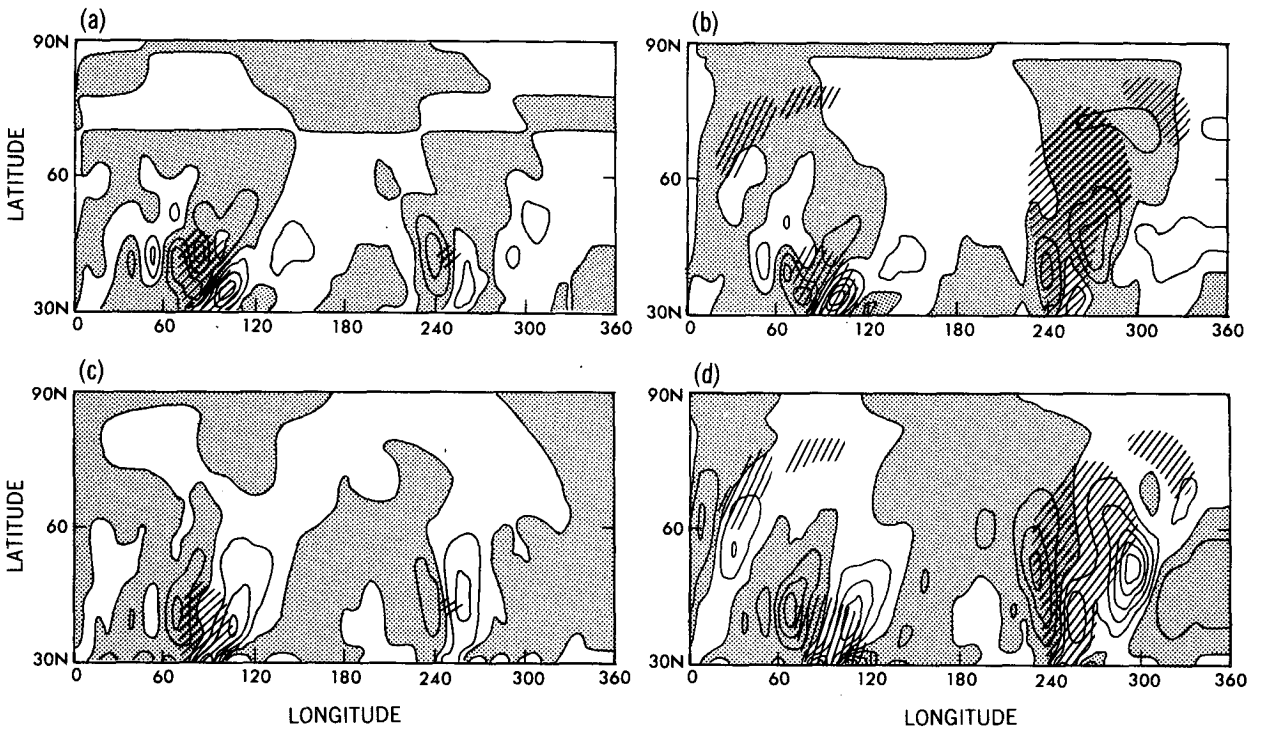

FIG. 11. Terms in the thermodynamic balance near the surface in the linear model: (a) first term, LHS of Eq. (3) for the present day case; (b) first term for the ice age case; (c) second term for the present day case; (d) second term for the ice age case. Hatching indicates topography above 1.5 km. Contour intervals are 1.5×10^{-5} K s^{-1}.

forced eddy fields from the linear model experiments for the present and ice age climates. The terms are computed near the surface at 990 mb. The first term is drawn in the figures on the top and the second term is on the bottom. Figures 11a and 11c are for the present day case, and Figs. 11b and 11d represent the ice age case. The plots are restricted north of the noisy critical latitude near 30°N. Cross hatching indicates where the surface is over 1.5 km as a reference. In the present day case (left figures), both terms are important near both centers of forcing, and the terms generally sum constructively. For the ice age case, $\bar{u}(\partial\Theta'/\partial\lambda)$ intensifies somewhat on the lee side of the Tibetan Plateau, and weakens upstream (Fig. 11b). In the western hemisphere, the map of $\bar{u}(\partial\Theta'/\partial\lambda)$ increases over the eastern slope of the ice sheet, but these changes are much less dramatic than the changes in $v'(\partial\bar{\Theta}/\partial\theta)$ which becomes the dominant term because the zonal mean meridional temperature gradient has doubled in this region.

Thus, in the western hemisphere, the adiabatic heating that occurs as air flows down the ice sheet toward the North Atlantic is balanced by the advection of cold air from the north by the eddy meridional velocity. This process is more important in the ice age climate than in the present day climate because the large change in the meridional gradient of the zonal mean temperature makes the import of cold Arctic air more efficient. Smaller eddy meridional velocities are required to balance the adiabatic warming because of this larger gradient in the ice age climate.

4. Conclusions and implications

A linearized, steady state, primitive equation model can provide a reasonable simulation of the stationary waves in a GCM with ice age boundary conditions. The presence of the ice sheets is the dominant cause of the change in stationary waves in the GCM. Since orographic features are represented in the linear model by a forcing proportional to the horizontal slope of the surface, but not as a physical presence that air must actually flow around as in the GCM, the resemblance degrades over land surfaces very near the surface. But this need not destroy the simulations at other levels or at low levels away from the orography, and we find that the Laurentide ice sheet in the linear model can produce strong subpolar North Atlantic cooling.

We are encouraged to use the linear model as a diagnostic tool to explore in more detail the physical mechanisms responsible for the GCM's response to ice age boundary conditions. Using the linear model analysis, we can separate the responses to orography, heating, and transient eddies to demonstrate that the mechanical effect of the changed slope of the surface—and not changes in the diabatic heating or the transient eddies that necessarily accompany the ice sheet in the GCM—is responsible for the ice sheets' influence on the stationary wave field.

Changes in the zonal mean climate state play an important role in how the stationary waves respond to the ice sheet forcing in the linear model. If the model is linearized about the GCM's present day basic zonal climate state instead of the ice age state, the amplitude of the glacier-induced stationary waves in the troposphere is roughly twice the amplitude of the waves that result when the ice age zonal mean climate is used. This effective damping of the stationary waves by the ice age zonal mean fields is due to the large change in the meridional temperature gradient, which doubles between 45° and 60°N in the ice age GCM climatology. During the ice age, cold polar air is closer to the area of adiabatic heating on the downslope of the Laurentide ice sheet and can be advected into the region by small eddy meridional velocities to balance the heating. The increased stability of the ice age atmosphere near the surface does not seem to be an important factor in determining the ice age stationary wave response.

It is surprising that the predictions of a linear theory are useful for an obstacle as large as the Laurentide ice sheet. We suspect that this may be related to the result from quasi-geostrophic theory that the steady linear response to orography is also a solution of the fully nonlinear equations if there is no meridional shear in the basic state zonal flow (e.g., Held 1983). Much work remains to be done to better define the limitations of linear theory in the presence of meridional shear.

Insofar as the subpolar North Atlantic cooling and changes in the tropospheric stationary waves are well simulated with linear dynamics, the linear model can be used to study the development of these features as a response to ice sheet growth or decay. Indeed, to the extent that linear theory is valid for this problem, one can conclude that the atmospheric circulation evolved in pace with the growing ice sheet and did not change abruptly as the ice sheet reached some critical size. While the present work suggests that linear theory is approximately valid, further studies of the nonlinear response to orography are needed to determine whether or not abrupt transitions are a possibility.

The problem is complicated by the sensitivity of the stationary waves to changes in the zonal mean basic state. Our results suggest that information about the time-evolution of the zonally averaged climate as well as the glacial orography is necessary in order to predict the time-evolution of the stationary waves. The changes in the mean meridional temperature gradient are probably more closely related to surface albedo changes rather than the changes in the height of the glacier. There could be a lag between, say, the time of the maximum magnitude of the meridional temperature gradient and maximum ice volume, leading to a complicated stationary eddy evolution.

Acknowledgments. We wish to thank S. Manabe, A. Broccoli, K. Bryan, D. Rind, J. Kutzbach, and S. Feldstein for their comments on this work. We also appre-

ciate the efforts of J. Kennedy in preparing the manuscript, and P. Tunison and staff in preparing the figures.

REFERENCES

Broccoli, A. J., and S. Manabe, 1987: The influence of continental ice, atmospheric CO_2, and land albedo on the climate of the last glacial maximum. *Cli. Dyn.*, **1**, 87–99.

Chen, S.-C., and K. E. Trenberth, 1988: Orographically forced planetary waves in the Northern Hemisphere winter: Steady state model with wave-coupled lower boundary formulation. *J. Atmos. Sci.*, **45**, 657–680.

CLIMAP Project, 1976: The surface of the ice-age earth. *Science*, **191**, 1131–1136.

——, 1981: Seasonal reconstructions of the earth's surface at the last glacial maximum. Geol. Soc. Am. Map Chart Ser., MC-36.

Charney, J., and A. Eliassen, 1949: A numerical method for predicting the perturbations of the middle latitude westerlies. *Tellus*, **1**, 38–54.

Gates, W. L., 1976: The numerical simulation of the ice age climate with a global general circulation model. *J. Atmos. Sci.*, **33**, 1844–1873.

Held, I. M., 1983: Stationary and quasi-stationary eddies in the extratropical troposphere: Theory. *Large-scale Dynamical Processes in the Atmosphere*, B. J. Hoskins and R. P. Pearce, Eds., Academic Press, 127–167.

Hoskins, B. J., and D. J. Karoly, 1981: The steady linear response of a spherical atmosphere to thermal and orographic forcing. *J. Atmos. Sci.*, **38**, 1179–1196.

Jacqmin, D., and R. S. Lindzen, 1985: The causation and sensitivity of the northern winter planetary waves. *J. Atmos. Sci.*, **42**, 724–745.

Kutzbach, J. E., and P. J. Guetter, 1986: The influence of changing orbital parameters and surface boundary conditions on climate simulations for the past 18,000 years. *J. Atmos. Sci.*, **43**, 1726–1759.

Lindeman, M., and J. Oerlemans, 1987: Northern Hemisphere ice sheets and planetary waves: A strong feedback mechanism. *J. Climate*, **7**, 109–117.

Manabe, S., and A. J. Broccoli, 1985a: The influence of continental ice sheets on the climate of an ice age. *J. Geophys. Res.*, **90**, 2167–2190.

——, and ——, 1985b: A comparison of climate model sensitivity with data from the last glacial maximum. *J. Atmos. Sci.*, **42**, 2643–2651.

Neftel, A., H. Oeschger, J. Schwander, B. Stauffer and R. Zumbrunn, 1982: Ice core sample measurements give atmospheric CO_2 content during the past 48,000 yr. *Nature*, **295**, 220–223.

Nigam, S., 1983: On the structure and forcing of tropospheric stationary waves. Ph.D. thesis, Princeton University, 203 pp.

——, I. M. Held and S. W. Lyons, 1986: Linear simulation of the stationary eddies in a GCM. Part I: The 'No Mountain' model. *J. Atmos. Sci.*, **43**, 2944–2961.

——, —— and ——, 1988: Linear simulation of the stationary eddies in a GCM. Part II: The 'Mountain' model. *J. Atmos. Sci.*, **45**, 1433–1452.

Rind, D., 1987: Components of the ice age circulation. *J. Geophys. Res.*, **92**, 4241–4281.

Shackleton, N. J., M. A. Hall, J. Line and C. Shuxi, 1983: Carbon isotope data in core V19-30 confirm reduced carbon dioxide concentration in the ice age atmosphere. *Nature*, **306**, 319–322.

Smagorinsky, J., 1953: The dynamical influence of large-scale heat sources and sinks on the quasi-stationary mean motions of the atmosphere. *Quart. J. Royal Meteor. Soc.*, **79**, 342–366.